Int J Adv Manuf Technol (2016) 83:835–845
DOI 10.1007/s00170-015-7640-y

ORIGINAL ARTICLE

Exploratory study of spiral NC tool path generation on triangular mesh based on local subdivision

Zixian Zhang · Yixiong Feng · Bingyin Ren · Ichiro Hagiwara

Received: 29 July 2014 / Accepted: 18 January 2015 / Published online: 31 July 2015

Abstract As a representation of free-form surface, triangle mesh model (commonly with the stereo lithography format) has gained wide application in CAD and CAM recently because of its simple geometric computation, superior robustness, and high efficiency in tool path generation. However, conventional tool-path generation methods for NURBS surface are incapable of direct application to mesh models. Development of a tool-path generation method based on mesh model with high machining precision is becoming a key problem for NC machining. In this paper, a spiral tool-path generation method in finish-cut process is developed based on the offset-surface method (also called cutter location method). A novel local subdivision method is proposed firstly to guarantee edges of the offset-mesh within the required tool-path interval, and then gouge-free tool-path is generated by organizing path through vertex of the offset-mesh. Therefore, all the path intervals are under precise control by the local subdivision, allowing the mesh surface with both steeper and flatter areas to be machined with high-precision. Besides, tool-path naturally runs along the boundary of the triangle mesh model, ensuring continuous cut for reducing the fluctuation of cutting load. At last, tool-paths with multiple connective areas are generated for several complex mesh surfaces to clarify efficiency and robust of proposed method.

Z. Zhang · I. Hagiwara
Department of Mechanical Science and Engineering, Tokyo Institute of Technology, Tokyo, Japan

Y. Feng (✉)
State Key Laboratory of Fluid Power Transmission and Control, Zhejiang University, Hangzhou 310027, China
e-mail: fyxtv@zju.edu.cn

B. Ren
Department of Mechanics, Harbin Institute of Technology, Harbin, China

Keywords NC machine · Local subdivision · Machining simulation · Tool interference · High precision

1 Introduction

Free-form surface is widely used in CAD and CAM [1], which are generally represented in two formats, algebraic surface (such as NURBS surface and B-spline surface), and polygon mesh. Triangle mesh model (commonly with the stereo lithography (STL) format) has gained wide application in CAD and CAM field recently because of its simple geometric computation, superior robustness, and high efficiency in surface intersection. However, conventional tool-path generation methods for algebraic surfaces are incapable of direct application to mesh models. Especially in reverse engineering, it is difficult to obtain perfect modeling data for complex surfaces using parametric surfaces [2] because construction of surface model with multi-patches sometimes can cause gaps between patches and the trimming operation is time consuming. Although Park [3] proposed methods for free-form surface with defects, the machining precision significantly decreases due to filling gaps. On the other hand, high quality triangular mesh can be easily obtained with high-efficiency and high-accuracy from the point cloud [4]. As triangle mesh becomes more and more popular in CAD and CAM, it can be provided by most CAD systems, and numerous algorithms for converting surface into triangular approximations have been proposed [5].

NC machining is a common manufacture method for free-form surface in mechanics, aeronautics, and even orthopedic surgery [6]. Various algorithms have been proposed and developed for NC tool-path generation on free-form surface, such as iso-parametric method [5], drive surface method [7], guide surface method [8, 9], G-buffer method [10], and curve-based approach. Although triangular mesh model is superior to the parametric surface in terms of gouge checking [11], almost all existing algorithms are proposed for conventional algebraic surface (B-spline, BURBS surface, etc.) and are incapable of direct application to mesh models. Excellent and robust NC path generation algorithm for triangle mesh is still insufficient for industrial application.

Iso-plane method [12] and iso-parameter method [5] are prevalent in NC tool-path generation, which are based on a constant tool-path interval or parameter in *u* or *v* direction of algebraic surface. In both methods, the tool-path interval cannot be adjusted according to the curvature of the local surface, leading to low machining precision of the work piece. Unevenly tool-path generation methods [13, 14] are proposed to overcome the problem by taking the curvature near cutter contact position (CL position) into consideration, but robust are still insufficient for complicated models with multiple connected areas.

Kim [15, 16] proposed the 2.5D contour parallel milling method for incomplete mesh model, which cannot be used for free-form surfaces. Jun and Dai developed [17, 18] the parallel tool path generation methods for polygon mesh model with free-form surface, which gained application in manufactory industry for their robust and simplicity. Xu [19] proposed a dual drive curve tool path planning method to guarantee the first-order continuity of machined surface. Lee [20] developed a tool-path generation method with a single setup change for propellers to improve the machining accuracy. However, in [17–20], the cutter runs in the Zigzag route resulting in uncontinuous tool-path, and the fluctuation of cutting load increases at the starting and ending position of a row. Lee [21] also proposed a Zig-Zag tool-path generation method for constant-scallop height based on mesh, which is applicable for the symmetry model. But it will become invalid for asymmetry model because tool-path interval varies with location; the last several row of tool-path will be irregular, leaving some blank areas cannot be planned.

Reversely, spiral tool path [14] runs continuously along the surface boundary, which can reduce the cutter retractions, tool wear, and machining time. Short tool life is still one bottleneck to widen HSM application [22] due to fluctuation of cutting load. Fortunately spiral tool-path can extend tool life to some extend by continuous cutting and minimizing the fluctuation of cutting load. However, robust spiral tool-path planning method for mesh surface is still insufficient, and existing methods for mesh model are also unable in control of tool-path interval according to surface curvature to get high precision.

In this paper, a spiral topology tool-path generation method is proposed to minimize cutting load fluctuation and improve machining precision for triangular mesh surfaces, based on the concept of controlling tool-path interval by a novel local subdivision method. The proposed method belongs to the cutter location (CL)-based method, and the offset mesh is calculated firstly as the cutter location surface. Offset mesh is adjusted by a novel local Loop subdivision method to ensure every edge within the required tool-path interval. Then gouge-free NC tool-path is generated by organizing path through vertices of the offset mesh to make all path intervals under precise control, which allows the sculptured surface incorporating both steeper and flatter areas to be machined with high-precision. Besides, tool-path runs naturally along the boundary of the triangle mesh model, thus tool path with the minimum tool retraction can be generated, resulting in substantial reduction of tool wear and machining time. Examination and tool-planning for blank areas are also proposed to make sure all mesh can be planned precisely.

In Section 2, loop subdivision method is introduced prior to illustration of the proposed novel local subdivision method. In Section 3, the novel spiral tool-path generation method is described in detail. To illustrate robust and efficiency of the proposed method, various complex mesh surfaces with multiple connective areas are conducted in Section 4, and compared to the Iso-plane method [12]. In Section 5, conclusion and future work of this research are discussed.

2 Local loop subdivision method

This section provides a preparation for path generation by locally subdividing offset surface of the triangular mesh recursively to guarantee all the edges of offset surface shorter than calculated path interval. Thus the scallop height between the adjacent two tool-paths is insured to meet the specified machining precision. In this section, loop subdivision surface is firstly introduced in brief prior to introduction of the novel local subdivision method. And the calculation method of desirable tool-path interval (which guarantee machining precision) based on local surface curvature and cutter parameter is given. The offset surface of the mesh surface model is generated by offset each vertex of the mesh model along the normal vector of the vertex, which is locally subdivided to ensure every edge within the required path interval.

2.1 Loop subdivision surface

Loop subdivision surface is defined as the limit of vertices of finer and finer controlled triangles generated by such a recursive way that old vertices are updated and new vertices are introduced in each step according to subdivision rules [23]. In each step of loop subdivision, two kinds of points should be considered: even vertices which are in the original triangular mesh surface, and odd vertices which are newly generated and inserted into original edges. Explicate formulas are provided to get new positions for both odd and even vertices. If loop subdivision is applied infinitely times, the control-mesh is prone to a smooth surface called limit surface with C2-continuity almost everywhere on the surface [24] except extraordinary vertices (whose adjacent vertices number is not six). Every vertex on the control mesh approaches to a corresponding point in the limit surface gradually, coordinate of which can be calculated by formula without any subdivision [25]. The significant advantage of the subdivision surface is to represent smooth surface of complex arbitrary topology in just one "single" patch without trimming and sewing operation (which is commonly necessary for NURBS surface construction). It also inherits many nice properties of its underlying B-spline [26].

2.2 Path interval

Tool-path interval is defined as the shortest distance between two adjacent NC tool paths, indicated by L in Fig. 2, which is of great importance to control the scallop height (the maximum thickness of the uncut volume) and affects the machining precision. Control of the tool-path interval is necessary for high machining precision.

The curvature of a specified point V_i of the mesh surface is calculated by Eq. 1, where A presents the sum area of triangles with the common convex of V_i; α_j and β_j are two angles corresponding to edge $\mathbf{E}_{ij}$, shown in Fig. 1.

$$\overline{\mathrm{k}} = \frac{1}{4\mathrm{A}} \sum_{j=1}^{n} \left(\cot\alpha_j + \cot\beta_j\right) \left|\mathrm{V}_j - \mathrm{V}_i\right| \quad (1)$$

Calculation of path interval can be presented as Eq. 2 by scallop height (h), cutter radius (r), and radius of surface curvature on the cutter contact (CC) position (R in Fig. 2), where R is positive if the surface is convex and negative if the surface is concave.

$$L = \frac{|R|\sqrt{4(r+R)^2(h+R)^2 - \left[R^2 + 2rR + (h+R)^2\right]^2}}{(r+R)(h+R)} \quad (2)$$

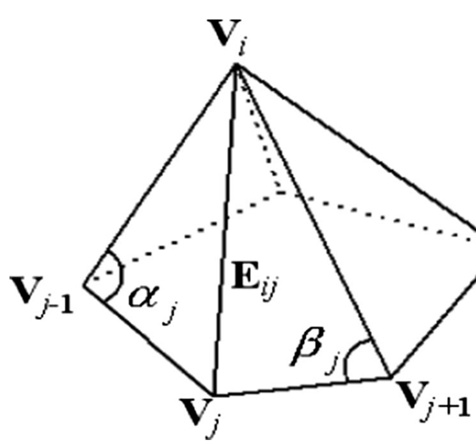

Fig. 1 Illustration of α_j and β_j

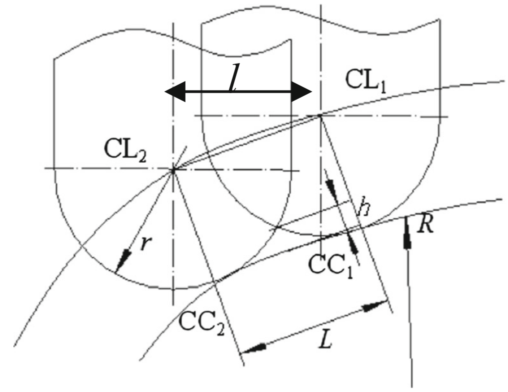

Fig. 2 Tool-path interval on free-form surface

Equation 2 can be simplified to Eq. 3 when radius of curvature R is much large than cutter radius r, and simplified to Eq. 4 when cutter radius r is much larger than scallop height h, so as to improve the calculation efficiency of proposed algorithm.

$$L = 2\sqrt{(2r-h)h} \quad (3)$$

$$L = \sqrt{\frac{8hrR}{r+R}} \quad (4)$$

2.3 Local subdivision of offset surface

The CL-based approach is applied for tool-path generation in the proposed algorithm. CL surface, which is also called guide surface in some literature, is a surface on which the cutter positions are limited on. Vertex of the mesh surface model is offset one by one along the normal vector of the vertex for a distance of mill radius r. These offset vertices are then connected according to their original topological relationships to form the offset mesh surface. The offset surface of a human face model is shown in Fig. 3. Local subdivision is applied on the offset mesh surface to adjust the length of mesh edges so as to control the tool-path interval and the scallop height.

All the triangles of the mesh model are saved in a triangle list in a certain order. From the beginning of the list, triangles are checked one by one until the edges of a triangle is found longer than the required tool-path interval. And the triangle should be subdivided according to the proposed local subdivision method shown in Fig. 4. The proposed method deals with three situations (Fig. 4) according to the number of edges larger than required tool-path interval.

In Fig. 4a, edge ab of triangle abc is longer than required tool-path interval, so additional vertex O is added between the

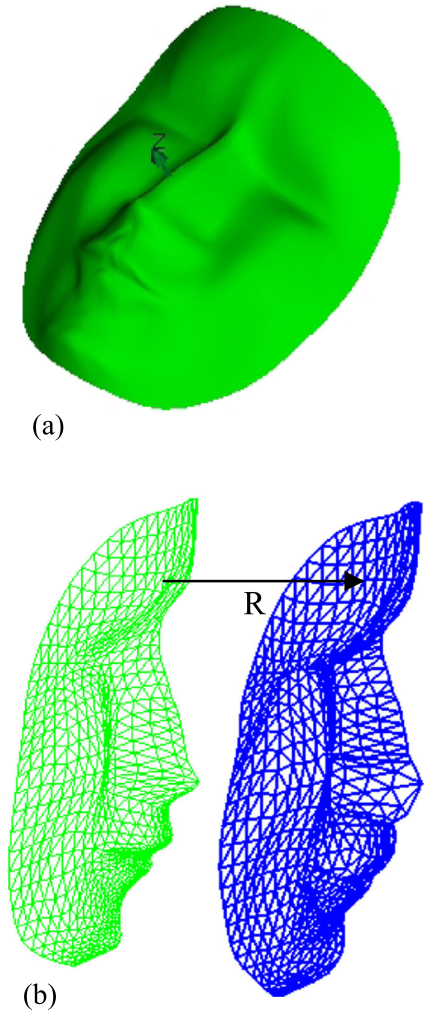

Fig. 3 Surface model of a human face and offset surface. **a** Face surface. **b** Triangular mesh of face model and its offset surface

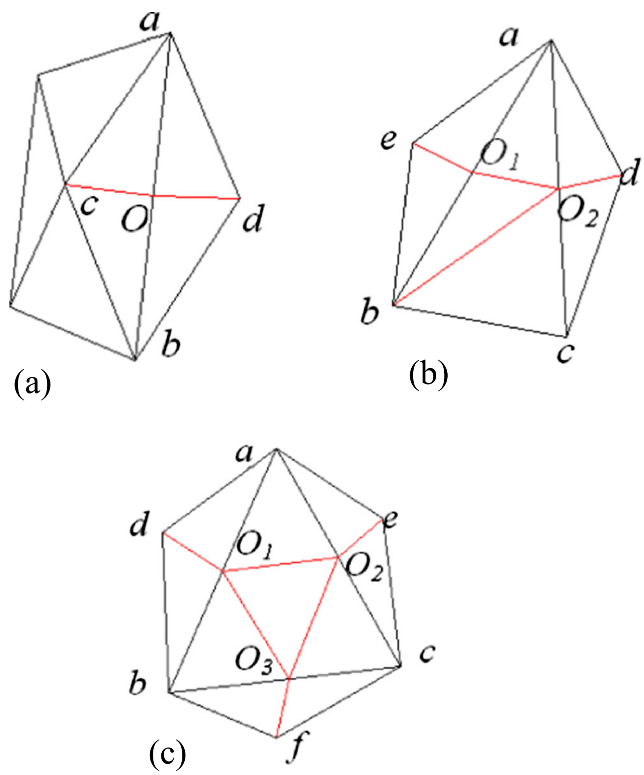

Fig. 4 Three types for local subdivision method according to number of edges longer than calculated interval. **a** Local subdivision method for triangles with one long edge. **b** Local subdivision method for triangles with two long edges. **c** Local subdivision method for triangles with three long edges

vertex a and b. Coordinate of the additional vertex O is defined by the weighted combination of local adjacent points of the mesh surface by Eq. 5, and weight of adjacent points is shown in Fig. 5a. Then coordinate of the even vertices (vertices of the mesh surface adjacent to the additional vertex) a, b, c, and d are updated by the weighted combination of local adjacent points. The weight of each adjacent vertex is calculated by Eq. 6 with n expressing number of vertices and O, a, b, c, and d expressing vertices coordination, shown in Fig. 5b [13].

$$\overrightarrow{O} = \frac{1}{8}\left(\overrightarrow{a} + \overrightarrow{b}\right) + \frac{3}{8}\left(\overrightarrow{c} + \overrightarrow{d}\right) \tag{5}$$

$$\alpha = \frac{1}{n}\left[\frac{5}{8} - \left(\frac{3}{8} + \frac{1}{4}\cos\frac{2\pi}{n}\right)^2\right] \tag{6}$$

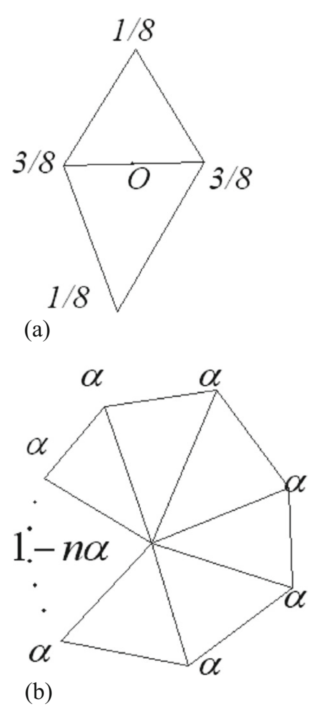

Fig. 5 Weights distribution for odd and even vertices. **a** Weights distribution for new vertex. **b** Weights for updating even vertices

Thus, the edge longer than the required tool-path interval is subdivided into two shorter edges, and two triangles *abc* and *abd* which contains edge *ab* are subdivided into four triangles *aoc*, *aod*, *boc*, and *bod*. To update the triangle list, the original two triangles *abc* and *abd* are deleted and newly generated four triangles *aoc*, *aod*, *boc*, and *bod* are inserted at the end of the triangle list.

In Fig. 4b, two edges of the triangle *abc* are longer than required tool-path interval, and additional vertices O_1 and O_2 are added on edge *ab* and *ac*. To update the triangle list, the original three triangles *abc*, *abe*, and *acd* are deleted and newly generated seven triangles are inserted at the end of the triangle list. In Fig. 4c, three edges of the triangle *abc* are all longer than the required tool-path interval, so three additional vertices O_1, O_2, and O_3 are added and ten smaller triangles are generated and inserted at the end of the triangle list.

After a triangle is subdivided, the next triangle in the triangle list is then checked to decide whether it should be subdivided or not. Local subdivision is applied recursively until all the edges of all triangles in the triangle list are within the calculated path interval. In Fig. 6, a convex mesh surface is local subdivided as an example, for which ball-end tool with radius of 8 is applied and the scallop height for are 0.05 (Fig. 6b), 0.04 (Fig. 6c), and 0.03 mm (Fig. 6d), respectively. From these examples, we can see that the higher machining precision is required, the shorter the interval should be and more edges are subdivided.

Tool-path interval and step length over the mesh surface are guaranteed to be under precise control by local subdivision method, so that the scallop height of work piece will satisfy the specified machining precision. In the proposed method, the direction L (Fig. 2) through CL positions O_1 and O_2 is exploited to adjust path interval, more precise than the distance *l* between adjacent drive planes which is used by most drive plane method [12]. This also contributes to higher machining precision, indicated by the simulation result in Section 4.

3 Spiral tool-path planning

Edges of built offset surface via local subdivision method are elaborately selected to construct tool-path according to proposed algorithm in this section. The following definitions are made firstly to facilitate the expatiation of the proposed algorithm.

Former Point: In the proposed method, vertices of offset surface are used as CL positions of the tool-path. The latest CL position of offset surface vertex is defined as Former Point indicated in Fig. 7b while searching a new cutter location (CL) position. In other words, once a vertex on the offset mesh is selected as a CL position, it becomes the Former Point for the next CL position.

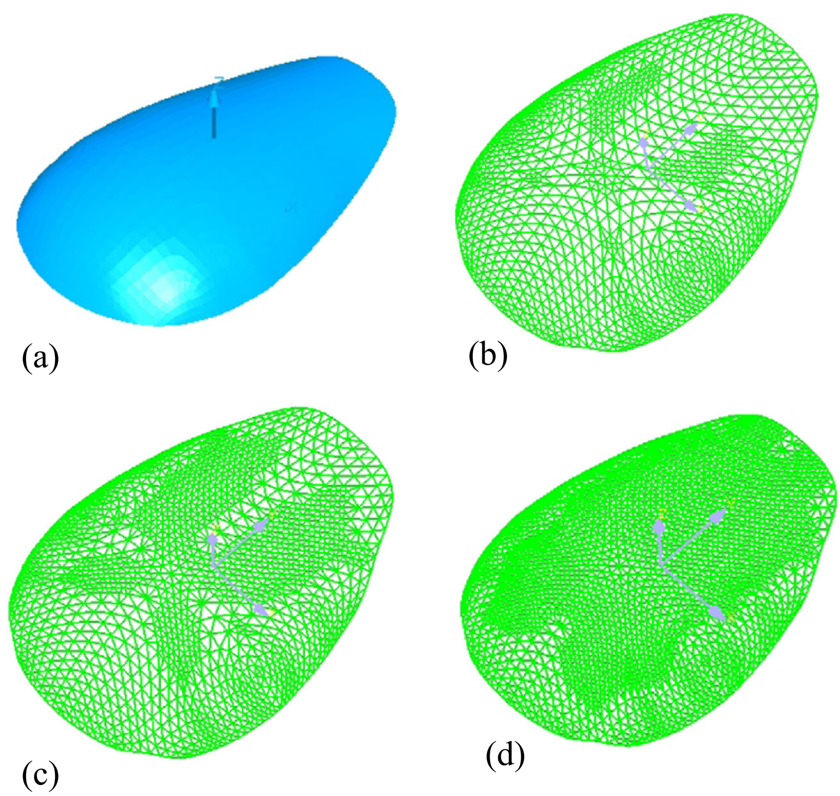

Fig. 6 Locally subdivided offset surface with different scallop height. **a** Convex surface. **b** Scallop height 0.05 mm. **c** Scallop height 0.04 mm. **d** Scallop height 0.03 mm

Former Row: The latest row of CL path is taken as Former Row to find a new cutter location (CL) position, shown in Fig. 7a.

Vertex of the offset surface in the proposed method contains two kinds of information, i.e., the coordinates of the point and an indicator to record whether this vertex has already been used as a CL point or not. The algorithm is realized in the C++ language, and the structure of vertex is designed with the following data format:

```
class vertex
{ public:
double x, y, z; //Coordinates
bool used; //Whether this vertex has already been used as a CL point or not.
}
```

The first step of tool-path planning is to generate the boundary tool-path by connecting boundary edges of offset surface in sequence, which mainly consists of three sub-steps.

1. Edge list of offset surface are judged until one edge is found as the boundary edge which only exists in one triangle of the offset surface. Then the two end points of the edge are labeled with used (used=true), saved to the Former Row list. One of the two end points is also saved to Former Point to search the next CL position.
2. Edges of offset surface are judged until the boundary edge, whose one end point is Former Point and the other is unused (the indicator of the vertex structure "used"==false), is found. The unused end point of the boundary edge is labeled with used (used=true) and saved as Former Point and Former Row list.
3. Sub-step 2 is repeated until the boundary edge with Former Point and an unused vertex can not be found. The boundary of offset surface is set as the first row of tool-path, and both Former Row list and Former point are also filled for the next row of tool-path.

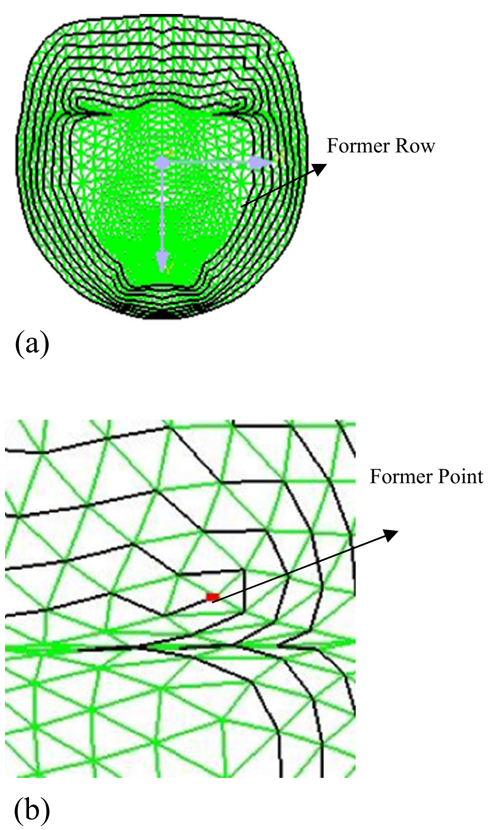

Fig. 7 Corner situation of tool-path for the face model. **a** Spiral tool-path with corner prevention. **b** Former Point

The generated boundary tool path, with Former Point and Former Row indicating the latest selected vertex on boundary and boundary vertices of offset surface, respectively, is applied to form the next row. As the beginning CL position of next row, proper vertex will be elaborately chosen according to the following rule: If one end of offset surface edge is the Former Point, and the other end is unused and can connect to Former Row through only one edge, the unused vertex should be selected to form the second row of tool-path. The brief procedure is shown as follows:

1. Vertex list of the offset surface are searched until a vertex, which is not used and can connect to Former Point only through one edge, is found as the starting location of the next row of tool-path. This vertex is labeled with used (used=true) and saved to Former Point.
2. Edges of offset surface are searched until one edge satisfying two requirements, i.e., (1) one end point of the edge is Former Point, and (2) the other end is unused (used=false) and connects to a vertex in the Former Row only through one edge. The unused vertex of the edge is selected as a new CL position, labeled with used (used=true), and saved into Former Point.
3. Repeat step 2 until no edge satisfying these two requirements exist. Then all the newly calculated CL positions are connected with each other to generate the second row of tool path, which is saved to Former Row overlaying the previous Former Row data, preparing for subsequent row.

Reviewing the method for calculating the second row, it is obvious that two requirements are necessary for calculation of new row of tool-path: a starting position (vertex) of the new row of tool-path and the Former Row. If these two requirements can be satisfied, tool-path can be planed row after row by the same method to generating the second row, until the these two requirements in step 2 can not be satisfied, which means all vertices which can connect to Former Point through only one edge are already used. In this case there are two possible situations: (1) tool-path has passed through all offset surface vertices and NC path generation is successfully finished and (2) the Former Point is arrested in a corner and cannot go out of the circle, shown in Fig. 7a, where the last vertex used for CL position is expressed in red in Fig. 7b.

Although unused vertices still exist in the surface in Fig. 7, all vertices which can connect to Former Point through only one edge are all used. Therefore, starting position (vertex) for a new row can not be found and tool-path generation cannot be continued by the same method to generate the next row of tool-path. So new method is proposed for founding the starting position and Former Row for this situation:

For calculating Former Row: The edge list of the offset surface is searched until find one edge consisting one used end point and one unused end point. The used end point is saved into Former Row overlaying previous data and the unused end point is saved to another data list called the Present Row, preparing for the next step.

For calculating staring position of the new row of tool-path: The Present Row is searched and if a vertex in Present Row is located in a corner (only one unused vertex can connect to it through only one edge), it is selected as the starting position of the new row of tool-path. If such vertex does not exist in the Present Row, then vertex in Present Row nearest to Former Point is used for starting position (vertex) and saved to Former Point overlaying the previous data.

Thus, the starting position and Former Row are both prepared, and the new row of tool-path can be generated using the same way as the second row of tool-path. However, in this case, distance between the starting position of the new row and the last CL position of the previous row of tool-path may be larger than calculated interval, and can not be regarded as one step length (Fig. 8). In order to solve the problem, two extra CL positions are added to lead tool-path ascend to a safe height in the *z* axis direction and connect to starting position of the new row, shown in Fig. 8. Then tool-paths are generated using the same way as the second row. If tool-path is trapped in a corner again, new starting position and Former Row should be searched until tool-path has passed through all vertices of offset surface.

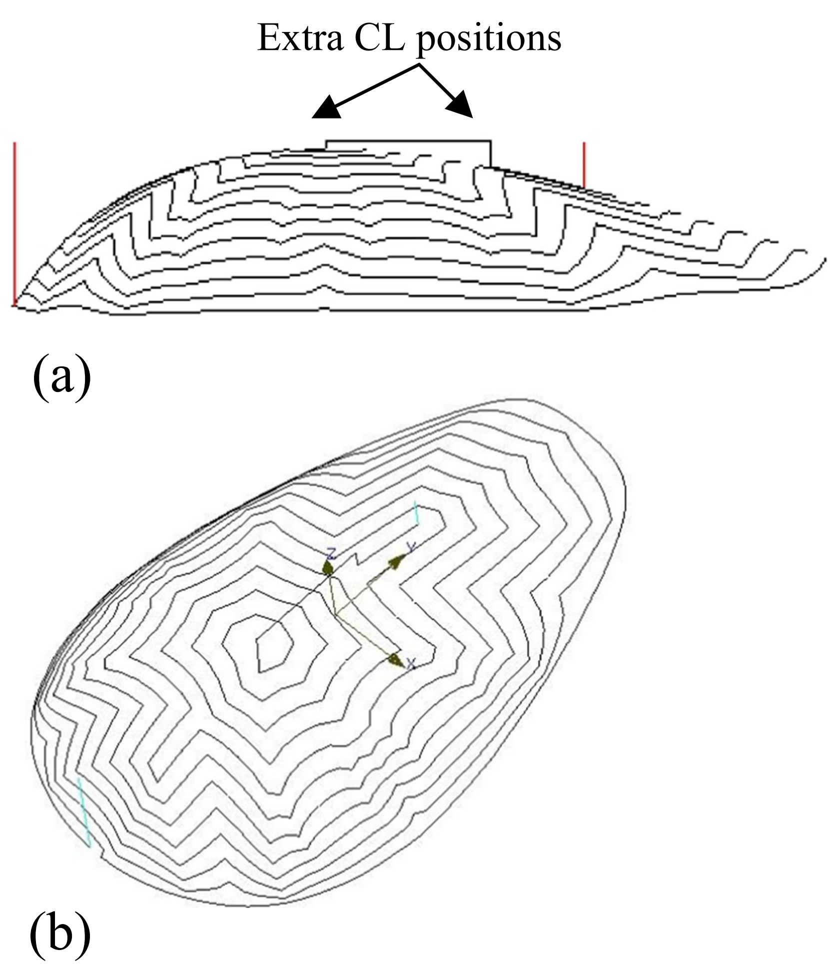

Fig. 8 Tool-path for multiple connected areas. **a** Left view. **b** Top view

In Fig. 9, NC tool-paths for the "face" model with different cutter radius and scallop height are provided as illustration examples. In Fig. 9d, starting position has been searched twice because locally subdivided surface is much more complicated than the original mesh.

After tool-path generation is finished, machining precision can be estimated in simulation (Section 4) by comparing the machined surface and the original mesh surface model. If over-cut is not within required precision, machining tool is changed and tool-path is calculated again, until available tool-path is obtained. The flowchart of the proposed method is shown in Fig. 10.

Machining precision of the proposed method is theoretically much higher than the parallel tool-path generation method [18], which is commonly used in NC machining. In the machining process on triangular mesh, largest under-cut appears in the bottom of the concave area probably, expressed by h in Fig. 11a. If the proposed method is applied, because the CL (cutter location) points are selected from the vertices of the offset surface, CC (cutter contact) points always pass the vertices of triangular mesh. Thus machining error is divided into

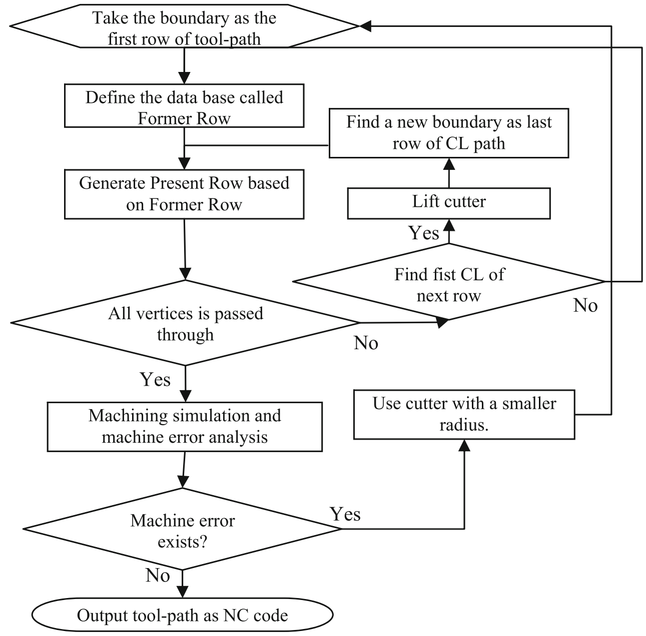

Fig. 10 Procedure of spiral tool-path generation

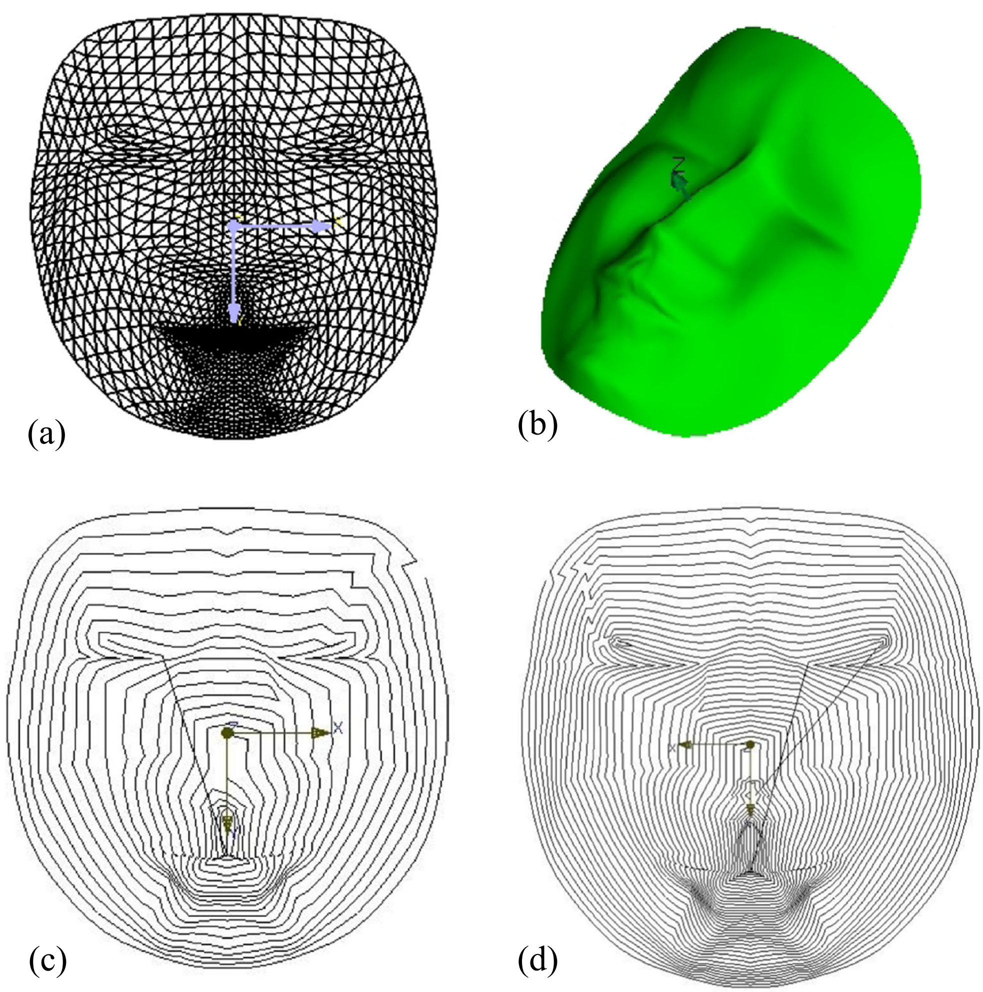

Fig. 9 Tool-path with different scallop height (cutter radius 2 mm). **a** Triangular mesh of face model. **b** Face surface model. **c** Tool-path with large scallop height (0.5 mm). **d** Tool-path with high scallop height (0.2 mm)

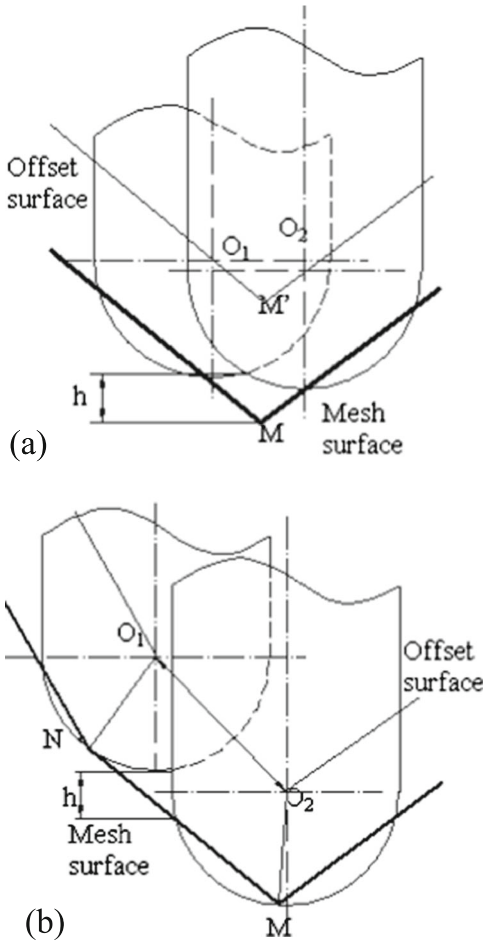

Fig. 11 CL position of the proposed method and drive-plane method. **a** CL position of drive plane method. **b** CL position of proposed method

under-cut (removed too little material) and over-cut (removed too much material), and the maximum scallop height is minimized (Fig. 11b), which will be clarified in the machining simulation in Section 4. However, maximum over-cut also appears in the bottom vertex of concave area, and when applying the proposed method CC (cutter contact) route passes all vertices of mesh model, thus the possibility of over-cut is increased substantially. Fortunately, this problem can be solved by applying cutters with smaller radius.

4 Machining simulation

Z-map method [12] is a widely used for machining simulation method to estimate the machining precision and the quality of NC tool-path, by comparing the machined surface and original mesh surface model. In this section, tool-paths are generated for three models (the concave model, convex model, and the "Face" model) by the proposed spiral tool-path generation method, and its efficiency and robust are verified by simulation of the machining process and machining results based on Z-map method. Tool-paths are also generated by parallel tool-path generation method [18] for the same three models and are

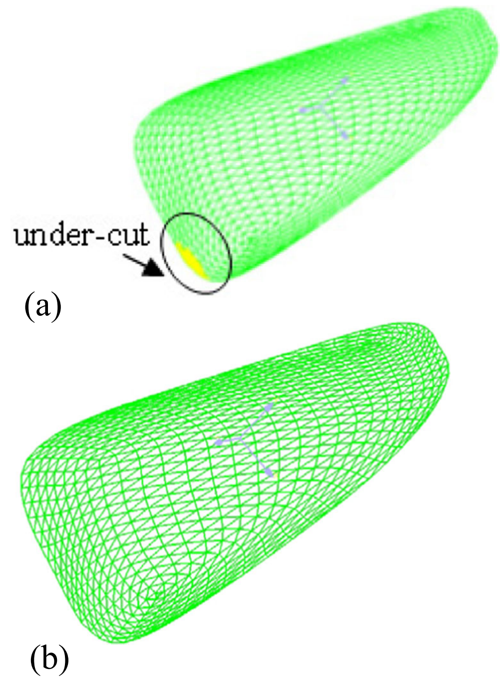

Fig. 12 Result of error analysis for concave surface. **a** Machining result of parallel tool-path generation with under-cut. **b** Machining result of spiral tool-path generation

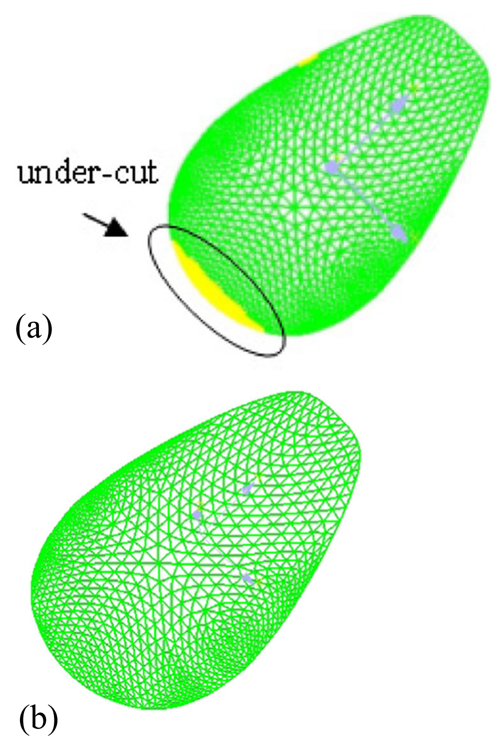

Fig. 13 Result of error analysis for convex surface. **a** Machining result of parallel tool-path generation. **b** Machining result of spiral tool-path generation

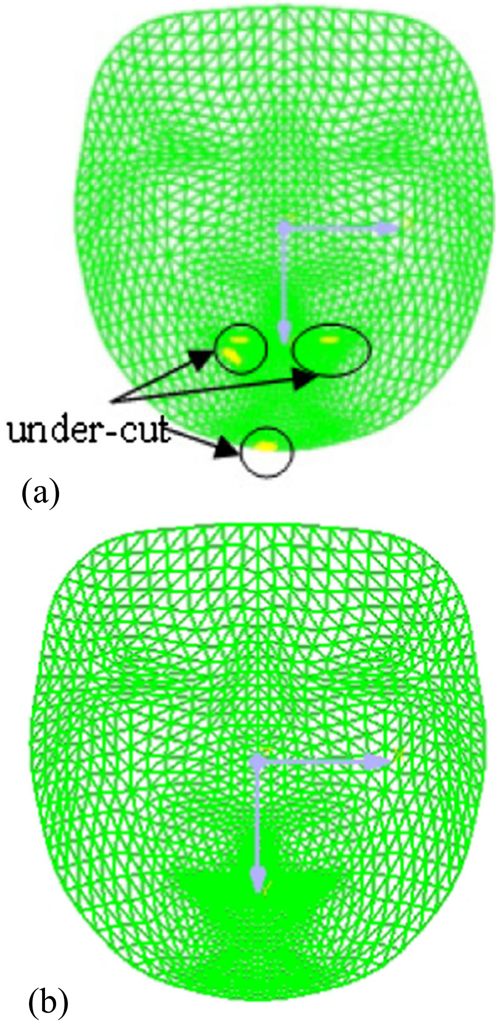

Fig. 14 Result of error analysis for face surface (cutter R1 mm). **a** Machining result of parallel tool-path generation. **b** Machining result of spiral tool-path generation

simulated in the same PC for comparison with the proposed method, shown in Figs. 11, 12, and 13.

In Figs. 12, 13, and 14, machining error is calculated as the distance between the machined work piece and the original mesh surface [12], and compared with the user specified allowance. If the machining error of some part of the machined work piece is larger than the specified allowance, this part of the work piece is expressed in yellow color, otherwise, is expressed in green color. The machining parameters for Figs. 12, 13, and 14 are listed in Table 1.

Fig. 15 Machining result of Face model

Figures 12a, 13a, and 14a are machining simulation results by the parallel tool-path generation method, and Figs. 12b, 13b, and 14b are result by the proposed spiral tool-path generation method. It is clear that with the same cutter and the same machining time, the machining precision of proposed spiral tool-path generation method is much higher than the parallel tool-path generation method [18]. Although two kinds of tool-path length is nearly same, the result of machining simulation by proposed method can satisfy specified precision and shown in all green color in Figs. 12b, 13b, and 14b, large area of under-cut (cutter too little shown in yellow color) has already appeared on the machining result by parallel tool-path generation method in Figs. 12a, 13a, and 14a.

The actual machining experiment was done in SIEMENS 802D machining tool using wax as experiment material. The machining result of mesh-based face shown in Fig. 15 perfectly agrees with the simulation results in machining accuracy and smoothness of cutting route, which indicate the robust and efficiency of proposed method. The whole surface is machined efficiently without blank areas, and the gouge free

Table 1 Parameter of tool-path and simulation result (mm)

	Method	Cutter radius	Scallop height	Length of tool-path	Required precision	Under-cut and over-cut
Concave surface	Drive plane	4	0.0019	2,112.19	0.08	0~0.208
	Proposed		0.05	2,098.12		–
Convex surface	Drive plane	4	0.0035	2,010.45	0.019	0~0.601
	Proposed		0.01	2,007.69		–
Face surface (cutter R1)	Drive plane	1	0.027	6,609.86	0.2	0~0.449
	Proposed		0.2	6,591.49		–

machining is also illustrated by the smooth machining experiment result.

5 Conclusions

In this paper, a spiral topology tool-path in finish-cut process was developed to improve machining precision and decrease fluctuation of cutting load by continuous machining. Offset-mesh of the designed model was optimized firstly based on the novel local subdivision method to ensure every edge within the required interval, and spiral gouge-free tool-path was generated by organizing path through vertices of the offset-mesh.

(1) All path intervals were under precise control to make high-precision machine of complex mesh surface with steeper and flatter areas possible.
(2) Tool-path runs naturally along the boundary of the triangular mesh model, thus, tool path with the minimum tool retraction is generated to remarkably reduce tool wear and machining time.
(3) The proposed method is also robust for complex mesh surfaces in which CL path with multiple connected areas.
(4) High efficiency and machining precision of the proposed algorithm were clarified in manner of machining simulation and cutting experiment by comparison with parallel tool-path generation method. However, the proposed method is limited in 3-axis machining tools, and algorithms for 4-axis and 5-axis machining tool will also be developed in the future.

Acknowledgments This work was supported by the National Natural Science Foundation of China (No. 51322506), Zhejiang Provincial Natural Science Foundation of China (No. LR14E050003), the National High-Tech. R&D Program of China (No. 2013AA041303), Innovation Foundation of the State Key Laboratory of Fluid Power Transmission and Control, and Zhejiang University K.P. Chao's High Technology Development Foundation. Sincere appreciation is extended to the reviewers of this paper for their helpful comments.

References

1. Derose T, Kass M, Truong T (1998) Subdivision surfaces in character animation. In: SIGGRAPH 98 Conference Proceedings, Annual Conference Series, 85–94
2. Wu P, Suzuki H, Kaze K (2005) Three-axis NC cutter path generation for subdivision with z-map. JSME Int J Ser C 48(4)
3. Park SC, Chang M (2010) Tool path generation for a surface model with defects. Comput Ind 61:75–82
4. Li L, Schemenauer N, Peng X, Zeng Y, Gu P (2002) A reverse engineering system for rapid manufacturing of complex objects. Robot Comput Integr Manuf 18:53–67
5. Sun YW, Guo DM, Jia ZY, Wang HX (2006) Iso-parametric tool path generation from triangular meshes for free-form surface machining. Int J Adv Manuf Technol 28:721–726
6. Sugita N, Nakano T, Kato T, Nakajima Y (2010) Tool path generation for bone machining in minimally invasive orthopedic surgery. IEEE/ASME Trans Mechatron 15(3)
7. Lai YL (2010) Tool-path generation of planar NURBS curves. Robot Comput Integr Manuf 26:471–482
8. Kim BH, Choi BK (2000) Guide surface based tool path generation in 3-axis milling: an extension of the guide plane method. Comput Aided Des 32:191–199
9. Hwang JS (1992) Interference-free tool-path generation in the NC machining of parametric compound surface. Comput Aided Des 24(12):667–676
10. Saito T, Takahasi T (1991) NC machining with G-buffer method. Proceedings of the 18th annual conference on Computer graphics and interactive techniques 25(4):207–216
11. Kim SJ, Yang MY (2006) A CL surface deformation approach for constant scallop height tool path generation from triangular mesh. Int J Adv Manuf Technol 28:314–320
12. Zhang ZX, Savchenko M, Hagiwara I, Ren B (2010) 3-axis NC tool path generation and machining simulation for subdivision surface of complex models. Int J CAD/CAM 10(1):1–9
13. Shan Y, Wang SL, Tong SG (2000) Uneven offset method of NC tool path generation for free-form pocket machining. Comput Ind 43:97–103
14. Lee E (2003) Contour offset approach to spiral tool-path generation with constant scallop height. Comput Aided Des 35:511–518
15. Kim HC (2010) Optimum tool path generation for 2.5D direction-parallel milling with incomplete mesh model. J Mech Sci Technol 24(5):1019–1027
16. Kim HC (2010) Tool path generation for contour parallel milling with incomplete mesh model. Int J Adv Manuf Technol 48:443–454
17. Jun CS, Kim DS, Park SY (2002) A new curve-based approach to polyhedral machining. Comput Aided Des 34:379–389
18. Dai J, Wang H, Qin K (2004) Parallel generation of NC tool paths for subdivision surfaces. Int J CAD/CAM 4(1)
19. Xu R, Chen Z, Chen W, Zhu J (2010) Dual drive cue tool path planning method for 5-axis NC machining of sculptured surface. Chin J Aeronaut 23:486–494
20. Lee CS, Lee JH (2010) Geometric modeling and tool path generation of model propellers with a single setup change. Int J Adv Manuf Technol 50:253–263
21. Lee SG, Kim HC, Yang MY (2008) Mesh-based tool path generation for constant scallop-height machining. Int J Adv Manuf Technol 37: 15–22
22. Narutaki N, Yamane Y, Hayashi K, Kitagawa T (1997) High-speed machining of in conel 717 with ceramic tools. Ann CIRP 46(1):57–62
23. Loop CT (1987) Smooth subdivision surface based on triangles. M.S. Thesis, Department of Mathematics, University of Utah
24. DeRose T, Kass M, Truong T (1998) Subdivision surfaces in character animation. Proceedings of the 25th annual conference on Computer graphics and interactive techniques 194–203
25. Zorin D, Schroder P (2000) Subdivision for Modeling and Animation. SIGGRAPH 2000 Course Notes ACM SIGGRAPH
26. Desbrun M, Meyer M, Schroder P, Barr AH (1999) Implicit fairing of irregular meshes using diffusion and curvature flow. Computer Graphics Proceedings, Annual Conference Series, ACM SIGGRAPH, Los Angeles, California, 317–324